High-spin states of ^{99}Ag and ^{100}Cd

W. F. Piel, Jr., C. W. Beausang, D. B. Fossan, R. Ma, E. S. Paul, P. K. Weng,* and N. Xu
Physics Department, State University of New York at Stony Brook, Stony Brook, New York 11794

G. Scharff-Goldhaber
Physics Department, Brookhaven National Laboratory, Upton, New York 11973
(Received 28 August 1987)

High-spin states of ^{100}Cd up to $J^\pi = 8^+$ and an excitation energy of 2.5 MeV were studied by means of the ^{64}Zn(^{40}Ca,2p2nγ)^{100}Cd reaction. The $J^\pi = 8^+$ state was found to be isomeric with a half-life of 73±5 ns. The proposed level scheme is in agreement with that proposed recently by Alber *et al.* and is discussed in terms of expectations for the spectrum of a unique "pseudomagic" nucleus, i.e., an isobar of doubly magic ^{100}Sn which possesses a hole pair (protons) and a particle pair (neutrons) away from the magic number 50. Simultaneously, the ^{64}Zn(^{40}Ca,3p2nγ)^{99}Ag reaction was observed to populate states of ^{99}Ag up to $J^\pi = (\frac{27}{2}^+)$. The excitation energies of both nuclides are compared to those found recently for the lighter isotones ^{96}Ru, ^{97}Rh, and ^{98}Pd, and the systematic structures of the $N = 52$ nuclides are discussed.

I. INTRODUCTION

The present study of high-spin states of ^{99}Ag and ^{100}Cd is a continuation of an effort[1,2] to study the level schemes of the $N = 52$ nuclides; the earlier studies had populated and identified high-spin states of ^{96}Ru (up to $J^\pi = 18^+$), ^{97}Rh (up to $J = \frac{31}{2}$), and ^{98}Pd (up to 16^+). One goal is to compare the excitation energies of the levels of odd-A ^{99}Ag to those of the neighboring even-even nuclides in order to gain insight as to what nuclear structures become yrast in the $N = 52$ system. Additional information may be obtained from a comparison of the level scheme of ^{99}Ag to those of the odd-A isotones ^{95}Tc and ^{97}Rh.

A second goal is to shed light on the process by which collective excitations are built up as nucleons are added to closed shells. The low-lying yrast excitations of the $N = 52$ nuclides cannot be easily understood in either the shell model, as can the $N = 50$ nuclides, or in a collective model, as can some aspects of the $N = 54$ nuclides. The new data reported here should be helpful in this regard.

A third goal is to study high-spin states close to the doubly magic nucleus ^{100}Sn. This mostly unstudied region is expected to have many of the interesting features that the region around ^{208}Pb has shown over the years and should contain new physics made manifest by the change in the relative number of neutrons and protons. In particular, the yrast band of ^{100}Cd is of interest since this nuclide is an isobar of doubly magic ^{100}Sn. A phenomenological study, undertaken a few years ago, of yrast bands of even-even nuclides showed that all yrast bands of pseudomagic nuclides show downward deviations from the predictions of the variable moment of inertia (VMI) model, at least for the $J^\pi = 6^+$ and 8^+ states.[3] The ^{100}Cd nuclide is the heaviest pseudomagic nucleus which possesses a hole pair ($\pi g_{9/2}$) and a particle pair ($\nu d_{5/2}$) away from the same magic number. Moreover, the study of this region of the Periodic Table challenges the experimentalist to discover new techniques for effectively producing neutron-deficient nuclides.

During the course of this work the yrast levels of ^{100}Cd were reported[4] for the first time by Alber *et al.* from the ^{46}Ti(^{58}Ni,2p2nγ)^{100}Cd reaction. The present level energies are in agreement with their results as will be seen below. In addition we have measured angular distributions and excitation functions for the first time and have refined the half-life of the 8^+ level. The ^{99}Ag nuclide has not hitherto been studied in beam, although a study[5,6] of the β^+-EC (where EC denotes electron capture) decay of ^{99}Cd had led to the identification of low-lying $1/2^-$ and $7/2^+$ excited states of ^{99}Ag in addition to two other low-spin states. Calculations done in this laboratory using the computer code CASCADE (Ref. 7) suggested that fusion-evaporation processes would populate either of these nuclides with a cross section which is only about 1–2 % of the total fusion cross section. A 2p2n evaporation channel seemed to be the optimum choice to study ^{100}Cd. Therefore, an array of four highly efficient fast-neutron detectors was constructed and used to enhance those γ rays associated with the evaporation of one or more neutrons at the expense of the more probable charged particle channels. Moreover, the neutron multiplicity information allowed a definitive assignment of transitions to ^{99}Ag. In addition, an array of four large germanium detectors with bismuth germanate (BGO) anticompton shields has recently become available in this laboratory. These two new detector arrays facilitated the search for weak transitions.

II. EXPERIMENTS

The reactions ^{64}Zn(^{40}Ca,3p2nγ)^{99}Ag and ^{64}Zn(^{40}Ca,2p2nγ)^{100}Cd were utilized to populate states

of ^{99}Ag and ^{100}Cd using ^{40}Ca ions produced by the Stony Brook Superconducting LINAC Facility. The ^{64}Zn target of 1.1 mg/cm^2 was enriched to 99.5% and backed by 35 mg/cm^2 of lead to stop the beam. The data reported here include γ-ray excitation functions, angular distributions, and γ-γ coincidences. Moreover, in order to search for the existence of isomeric levels, the time delays between neutrons and γ rays were also recorded in a separate experiment. Germanium detectors, *n* type with an efficiency of 25% relative to a 7.6 cm$\times$7.6 cm NaI(Tl) detector for 1.33 MeV γ rays, were used. Each detector was inserted into a bismuth germanate anticompton shield of the transverse type.[8] The suppression of Compton scattering events from a detector was accomplished by vetoing the germanium timing signal, provided by a constant fraction discriminator, with a 500 ns wide pulse provided by the BGO shield. The suppression factor, averaged over energy, of each shield was about 6 for 1.33 MeV γ rays.

The γ-ray angular distributions were recorded both in singles mode and in coincidence with a neutron. The singles data were expected to offer good statistics while the neutron gated spectra should have had fewer transitions with a higher probability of resolving the transitions of interest. The spectra were recorded by positioning a Compton suppressed germanium detector successively at each of four angles measured with respect to the beam direction: 90°, 110°, 135°, and 148°. Two methods of relative normalization were used. One used the integrated charge of the beam hitting the target. The second utilized a fixed germanium detector located at $-90°$ to monitor the γ rays above 600 keV. The two methods were found to agree to 2.2% and the average of the two normalizations was used to extract the results. A ^{152}Eu source was subsequently placed at the target position to check that the beam spot had been at the center of rotation of the moving detector. This resulted in an average correction of 3.9% to the relative normalization at each angle. The sum of the singles spectra at all four angles produced by 167 MeV ^{40}Ca + ^{64}Zn is shown in Fig. 1. The production of several residual nuclides is apparent.

For the γ-γ coincidence experiments, four germanium detectors with BGO anticompton shields were used.[8] The interaction of direct γ rays from the target with the BGO was reduced by using 2.5 cm thick lead collimators. The centers of the detectors were located at $\pm 57°$ and $\pm 136°$ with respect to the beam direction and 14.2 cm from the target. A γ-γ coincidence was defined by the overlap of two 50 ns wide logic pulses, one from each detector, in a multiplicity logic unit. The γ-γ coincidence data were event-mode recorded onto magnetic tape. The magnetic tapes were subsequently scanned off line on a VAX 11-780 computer. The data from all six possible coincident pairs of detectors were summed into a 2048$\times$2048 channel array of E_γ vs E_γ. By storing the data in a symmetric mode, only one half of the array was required. Fine tuning of the gain of each detector was achieved by software during the scanning of tapes. Individual background-subtracted γ-ray gates could then

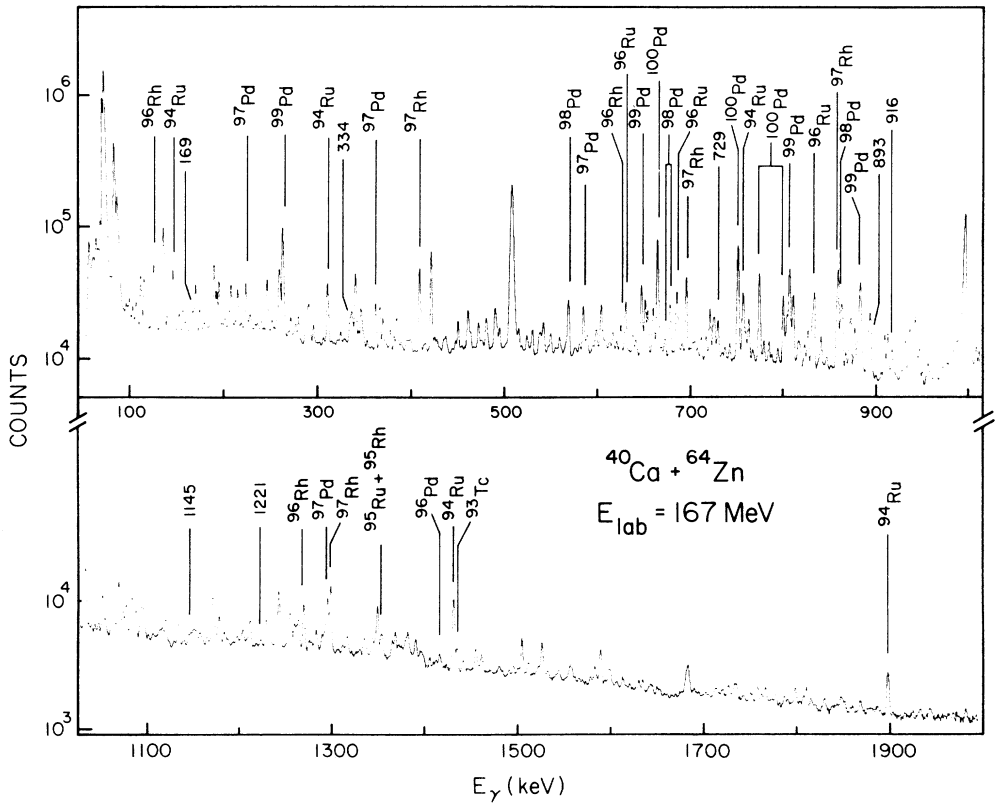

FIG. 1. Summed angular distribution singles spectrum produced by 167 MeV ^{40}Ca+^{64}Zn. The ^{99}Ag transition energies are labeled in keV. Several previously assigned transitions are labeled by nuclide.

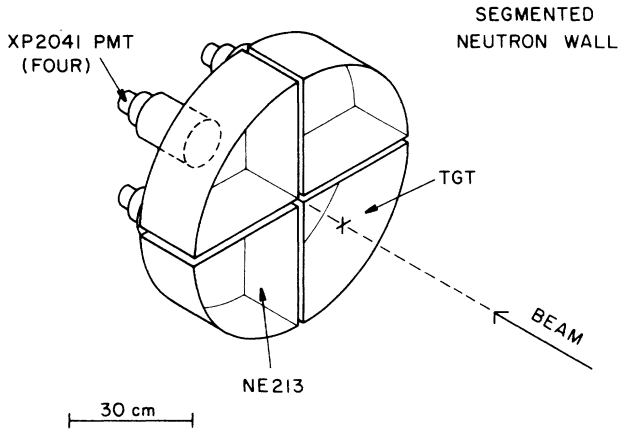

FIG. 2. Array of four neutron detectors. Each contains 10 liters of NE213 liquid scintillator and is optically connected to an Amperex XP2041 11 cm photomultiplier tube. A 2.5 cm thick layer of lead placed between the target and the detectors attenuated the gamma rays relative to the neutrons. In the present experiments, the detectors were separated by 5 cm of paraffin wax in order to minimize the scattering of neutrons from any one detector to another.

be conveniently formed from this array.

The evaporated neutrons were detected by an array of four NE213 liquid scintillator detectors centered about $\theta_{lab}=0°$ and subtending a total solid angle of 4.7 sr, as shown in Fig. 2. As shown by the dashed line in Fig. 2, the center of the upstream side of the detector array is located 10 cm behind the target. The intensity of γ rays striking the scintillator was reduced by a 2.5 cm thick layer of lead. About 97% of the surviving γ-ray events were distinguished from neutrons by means of electronic pulse shape discrimination. Gamma rays gated by the remaining 3% of the events were subsequently subtracted from the germanium spectra by a procedure which is described below. The four scintillators were separated by 5 cm of paraffin wax to minimize the scattering of neutrons from one to another. A γ-ray spectrum gated by one neutron is shown in Fig. 3(b) and a spectrum gated by two neutrons is shown in Fig. 3(a). Both spectra were produced by 167 MeV ^{40}Ca + ^{64}Zn. The spectra shown in Fig. 3 are the sums of spectra which were simultaneously recorded by two Compton suppressed germanium detectors located at $\pm 136°$ and have undergone corrections as described below.

The first correction made to the spectra in both Figs. 3(a) and (b) was to subtract the events due to γ rays striking the liquid scintillator. This was necessary since, as mentioned above, the γ rays were not completely discriminated against. Therefore, in a separate experiment a germanium spectrum was recorded with a time to amplitude converter (TAC) gate, which is normally set on the neutron peak, temporarily moved to the γ-ray peak. A subsequent channel by channel subtraction of this germanium spectrum, after being multiplied by a constant, from the raw one-neutron (1n) gated spectrum yielded the spectrum shown in Fig. 3(b). The value of the constant was determined by the requirement that transitions in ^{100}Pd, produced by the four proton evaporation channel, should not appear in this spectrum. This subtraction removed 30% of the counts from the raw 1n-gated spectrum and 28% from the raw 2n-gated spectrum.

The 2n-gated spectrum shown in Fig. 3(a) has in addi-

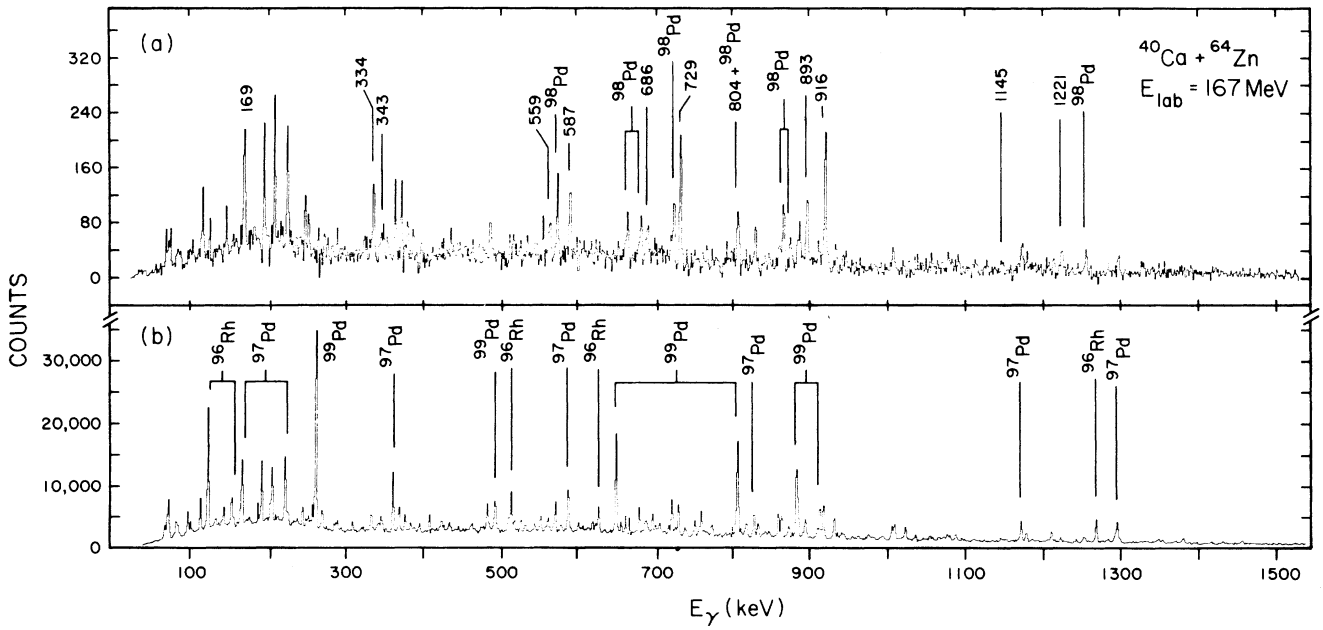

FIG. 3. (a) A germanium γ-ray spectrum observed in coincidence with two neutrons and produced by 167 MeV ^{40}Ca+^{64}Zn. This spectrum has been corrected for neutron scattering as discussed in the text. The lines presently assigned to ^{99}Ag are labeled by energy (in keV) and six of the strongest peaks in ^{98}Pd are also indicated. (b) A spectrum in coincidence with one neutron. Several peaks in ^{96}Rh (α3pn), ^{97}Pd (α2pn), and ^{99}Pd (4pn) are indicated.

tion been corrected for neutrons scattering from one NE213 segment to another, thereby causing both to trigger. This additional correction is accomplished by subtracting the 1n-gated spectrum in Fig. 3(b), multiplied by another constant f, from the 2n-gated spectrum. The constant f is determined by requiring that the photopeaks of γ-ray transitions known to be due to channels evaporating one neutron should not appear in the final 2n-gated γ-ray spectrum. The channels utilized were ^{99}Pd(4pn) and ^{96}Rh(α3pn). The value of the constant used was $f=0.0145\pm0.0008$, which removed 59% of the remaining counts, yielding the corrected spectrum shown in Fig. 3(a). We remark that there are transitions known to occur in other single neutron channels which were not completely removed from the 2n-gated spectrum shown in Fig. 3(a) by the above procedure. These channels and the corresponding value of the constant f are ^{97}Pd [α2pn, 0.0256(19)], ^{100}Ag [3pn, 0.022(5)], and ^{101}Cd [2pn, 0.032(8)]. Therefore, the value of the required constant seems to increase as the number of evaporated particles decreases.

The efficiency of the scintillator array for detecting a single neutron was found to be 11% from a comparison of the photopeak intensities of γ rays, from a 1-neutron channel, in a singles spectrum to a 1n-gated spectrum. Similarly, by utilizing transitions in ^{99}Ag, produced by the 3p2n channel, the efficiency of the scintillator array for detecting a "second" neutron was found to be 4% by comparing the photopeak intensities of each transition in the 2n-gated and 1n-gated spectra. This latter efficiency is smaller than one half of 11% because of the possibility of both neutrons hitting the same segment, yielding an apparent 1-neutron event. Finally, the efficiency for detecting a single neutron increases from 11% to 19% if the paraffin wax is removed and the four scintillator segments are brought together. These two numbers are decreased due to the use of the 2.5 cm thick lead shield but are increased by the kinematic forward peaking of neutrons and depend on the electronic adjustments made during each experiment.

III. RESULTS

The systematic behavior of the even-A nuclides with either 54 or 56 neutrons suggested that the energy spacings between the 0^+, 2^+, 4^+, 6^+, and 8^+ levels of $^{100}Cd_{52}$ should be similar to the analogous spacings in the isotone $^{94}Mo_{52}$. Therefore, the $2^+\rightarrow0^+$ transition in ^{100}Cd was expected to appear in the 2n-gated spectrum shown in Fig. 3(a) near the energy of the analogous ^{94}Mo transition, i.e., 871 keV, while the $4^+\rightarrow2^+$ transition should have appeared near 703 keV. An inspection of Fig. 3(a) reveals the presence of two intense transitions at 729.4 and 915.9 keV. These two transitions are observed to be in coincidence in the γ-γ coincidence data. Moreover, these two transitions are found to be the most intense transitions of a level scheme which is discussed below. In addition, a 1004.0 keV transition appears in Fig. 3(a) and has been assigned to be the $2^+\rightarrow0^+$ transition in ^{100}Cd by Alber *et al.*[4] Calculations performed using the computer code CASCADE suggested that transitions from only either ^{99}Ag or ^{100}Cd should appear in a 2n-gated spectrum, except for the known transitions in ^{98}Pd produced by the 2p4n channel. In order to seek further evidence concerning the transitions, the excitation functions were used.

The excitation function for the 915.9 keV transition, normalized to the empirical intensity of ^{100}Pd produced by the four proton evaporation channel, is shown in Fig. 4. The intensity of the $2^+\rightarrow0^+$ transition produced by the ^{100}Pd channel is estimated by taking 1.89 times that of the 798.6 keV $8^+\rightarrow6^+$ transition. This procedure removes any effect of feeding from the β^+-EC decay of ^{100}Ag to the 2^+ level of ^{100}Pd. This factor (1.89) was determined from previous (HI,xnγ) studies of ^{100}Pd where the simultaneous production of ^{100}Ag was not possible. The excitation functions which were calculated[7] using CASCADE, normalized to ^{100}Pd and corrected for the thickness of the target, are also shown in Fig. 4. The empirical excitation function of the 915.9 keV transition is similar to the curve expected for ^{99}Ag and unlike the curve for ^{100}Cd. Therefore, we assign the level scheme built upon the 915.9 keV transition shown in Fig. 5 to ^{99}Ag, produced by the 3p2n channel and discussed below. The summed spectrum of four background-subtracted γ-γ gates for ^{99}Ag is shown in Fig. 6(b).

The excitation function for the 1004.0 keV transition could not be obtained from singles spectra because of the presence of unresolved transitions in ^{96}Rh and ^{95}Rh produced by the α3pn and 2αp (or α3p2n) evaporation channels, respectively. Therefore, Fig. 4 shows the average intensity of the 795.0- and 452.6-keV transitions which were reported[4] to be the $4^+\rightarrow2^+$ and $6^+\rightarrow4^+$ transitions, respectively, in ^{100}Cd. These data might be expected to underestimate the ^{100}Cd production slightly due to side feeding into the 2^+ and 4^+ levels. However,

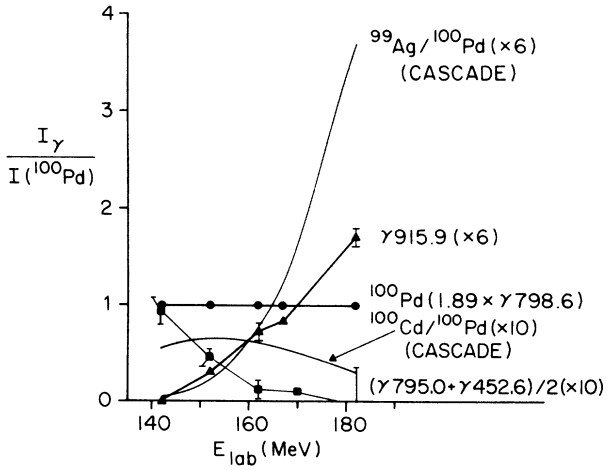

FIG. 4. Empirical γ-ray excitation functions, relative to ^{100}Pd, produced by ^{40}Ca+^{64}Zn. Two calculated curves which have been corrected for the present target thickness are also shown. The intensity of the 915.9 keV transition is to be compared to the calculated curve for ^{99}Ag while the average intensity of the 795.0- and 452.6-keV transitions is to be compared to the curve for ^{100}Cd. The intensity ratios have been multiplied by either six or ten in order to facilitate their display.

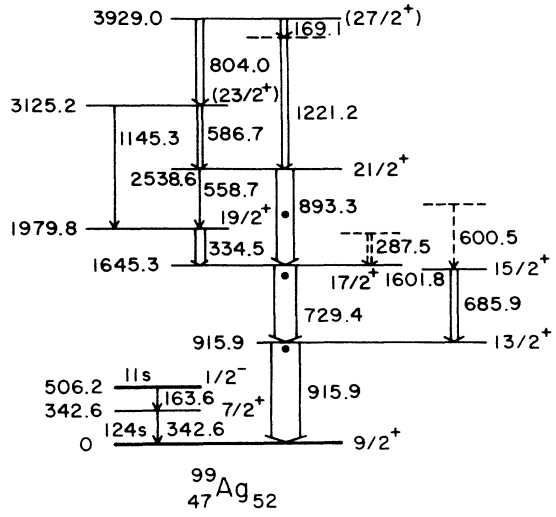

FIG. 5. Proposed level scheme for ^{99}Ag. The low-spin levels shown on the lower left were found in a β-decay study (Ref. 5). The black circles indicate the excitation energies of the 2^+, 4^+, and 6^+ states of the core nuclide ^{98}Pd. The γ-ray intensities are indicated by the width of the arrows.

since such transitions have not been found, perhaps the data shown in Fig. 4 account for at least 80% of the $2^+ \rightarrow 0^+$ intensity. The agreement with the curve, calculated using CASCADE shown in Fig. 4 is not conclusive. Therefore, we cannot confirm, from the present excitation function data, the ^{100}Cd assignment of Alber *et al.*[4] but simply adopt their conclusion. The summed spectrum of four background-subtracted γ-γ gates for ^{100}Cd is shown in Fig. 6(a). The expectation obtained from calculations using CASCADE that high-spin states of ^{99}Ag should be produced about 3.7 times more intensely (10.4 mb/2.8 mb=3.7) than those of ^{100}Cd can be checked by utilizing the γ-γ coincidence data. By setting a gate on the 1004.0 keV transition in ^{100}Cd, the intensity of the 795.0 keV transition was found. Similarly, by setting a gate on the 915.9 keV transition in ^{99}Ag, the summed intensity of the 729.4- and 685.9-keV transitions can be found. From these data, the ratio of ^{99}Ag to ^{100}Cd production at 167 MeV is 3.2±0.9 in agreement with the expected value.

In order to obtain information about the multipolarity of each transition of ^{99}Ag and ^{100}Cd, the formula

$$W(\theta)=A_0+A_2P_2(\theta)+A_4P_4(\theta) \quad (1)$$

was fitted to the observed γ-ray intensity function $W(\theta)$, where θ is the angle of the detector measured with respect to the beam direction, A_0, A_2, and A_4 are adjustable parameters, while P_2 and P_4 are Legendre polynomials. The intensity $W(\theta)$ is obtained for each transition by subtracting the Compton background from the intensity under the photopeak. The results of the fitting procedure are listed in Tables I and II for ^{99}Ag and ^{100}Cd, respectively. A slight correction was made to each A_2/A_0 and A_4/A_0 ratio for the finite solid angle subtended by the germanium detector. The A_0 values were corrected for the efficiency of the detector and normalized to the $13/2^+ \rightarrow 9/2^+$ transition for ^{99}Ag, or the $4^+ \rightarrow 2^+$ transition for ^{100}Cd, to obtain the relative γ-ray intensities. For several of the weaker transitions, the uncertainty in the A_4/A_0 value was large. Therefore, for these transitions, the parameter A_4 was set equal to zero and the fit was repeated in order to extract a value for A_2/A_0.

The yrast spin-parity assignments for ^{99}Ag shown in Fig. 5 seem straightforward up through the $J^\pi=21/2^+$ level. The $13/2^+ \rightarrow 9/2^+$ and $17/2^+ \rightarrow 13/2^+$ transition energies are found to be similar to the $4^+ \rightarrow 2^+$ and $2^+ \rightarrow 0^+$ transition energies in ^{98}Pd as indicated by the black circles in Fig. 5. This suggests a spectator role for a $g_{9/2}$ proton when coupled with the 2^+ or 4^+ (predom-

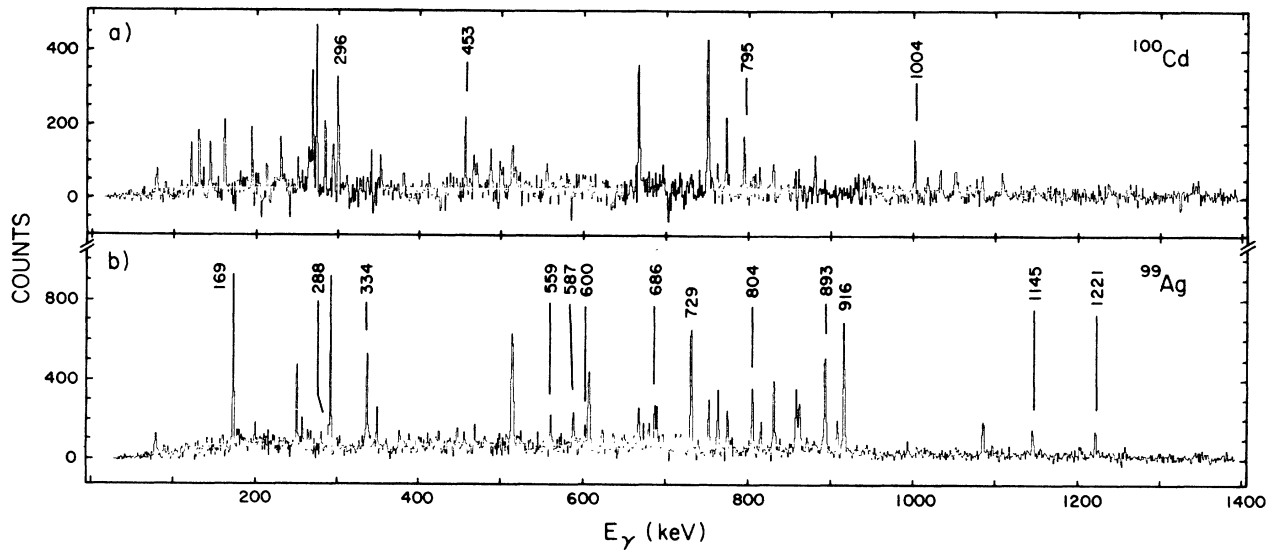

FIG. 6. (a) Sum of four background-subtracted γ-γ gates set on ^{100}Cd transitions: 1004.0, 795.0, 452.6, and 296.3 keV; (b) Similarly for four ^{99}Ag transitions: 915.9, 729.4, 334.5, and 1221.2 keV. The transitions assigned to each nuclide are labeled by their energies (in keV).

TABLE I. Transitions in ^{99}Ag. The relative γ-ray intensities and the angular distribution results are obtained from neutron-gated spectra and include a small correction for the finite solid angle of the germanium detector.

E_γ (keV)	I_γ	A_2/A_0	A_4/A_0	Assignment
163.6				$1/2^- \rightarrow 7/2^+$
169.08±0.25	11.0±0.4	−0.15±0.11	0.17±0.20	$(27/2^+ \rightarrow)$
287.54±0.20	9.9±0.6	−0.36±0.14	≡0	$(\rightarrow 17/2^+)$
334.53±0.20	26.7±1.0	−0.23±0.11	0.02±0.21	$19/2^+ \rightarrow 17/2^+$
342.6				$7/2^+ \rightarrow 9/2^+$
558.74±0.20	8.5±0.8	0.32±0.22	≡0	$21/2^+ \rightarrow 19/2^+$
586.71±0.25	14.7±4.7 [c]	[b]	[b]	$(23/2^+) \rightarrow 21/2^+$
600.49±0.30	17.7±1.5	0.72±0.26	≡0	$(\rightarrow 15/2^+)$
685.88±0.45	21.9±1.2	−0.20±0.24	≡0	$15/2^+ \rightarrow 13/2^+$
729.40±0.15	69.6±3.2	0.25±0.07	−0.10±0.13	$17/2^+ \rightarrow 13/2^+$
804.03±0.35	13.0±0.9	0.24±0.30	≡0	$(27/2^+) \rightarrow (23/2^+)$
893.29±0.25	49.7±2.6	0.33±0.08	0.04±0.15	$21/2^+ \rightarrow 17/2^+$
915.88±0.15	≡100.0±1.9 [a]	0.39±0.06 [a]	0.01±0.11 [a]	$13/2^+ \rightarrow 9/2^+$
1145.28±0.30	9.3±1.0	−0.12±0.25	≡0	$(23/2^+) \rightarrow 19/2^+$
1221.19±0.15	13.9±1.3	0.34±0.22	≡0	$(\rightarrow 21/2^+)$

[a]Value obtained from singles spectra with better statistical accuracy.
[b]Transition unresolved from a ^{97}Pd transition.
[c]Intensity obtained from γ-γ coincidence data.

inantly two-neutron) configurations of the lighter even-even $N=52$ neighbor to the maximum possible spin. It is noteworthy that no $21/2^+$ level of ^{99}Ag is found at an excitation energy near that of the 6^+ level of ^{98}Pd as indicated in Fig. 5. As was pointed out in Ref. 1, the $6^+ \rightarrow 4^+$ energy spacing in ^{98}Pd is larger than expected in the context of the shell model for the $\nu g_{7/2}^2$ (or $\nu d_{5/2} g_{7/2}$) configuration. The failure to observe a candidate spectator-proton state with $J^\pi = 21/2^+$ in ^{99}Ag at about 2.11 MeV suggests that the 6^+ state in ^{98}Pd includes an important contribution from configurations of $\pi g_{9/2}^{-4}(\nu=2)$ coupled to the two valence neutrons.

A sequence of states with $J^\pi = 19/2^+$, $21/2^+$, and $(23/2^+)$ is shown in Fig. 5, ranging from 1979.8 to 3125.2 keV. These states are connected by three transitions which are probably $M1/E2$ and an $E2$ cross-over transition. These levels may involve $\pi g_{9/2}^{-3}(\nu=1) \times \nu h_{11/2}^2$ configurations which can achieve a maximum spin parity of $J^\pi = 29/2^+$. However, the irregular sequence of the $M1$ transition energies may be an indication of strong admixtures of competing configurations. A candidate structure is the $\nu=3$ configuration of $\pi g_{9/2}^{-3}$ with $J^\pi = 21/2^+$. Another admixture, especially to the $21/2^+$ level, may be the $\pi g_{9/2} \nu d_{5/2} g_{7/2}$ configuration as discussed below. The ordering of the 1221.2- and 169.1-keV transitions could not be determined. Therefore, the level between them is dashed in Fig. 5. On the right side of Fig. 5 is shown the 685.9 keV transition. The level at 1601.8 keV can only have a spin of $\frac{15}{2}$ since if the spin were instead $\frac{13}{2}$, a transition to the $9/2^+$ ground state would have been expected, in contrast to the upper limit of 1.8 ($I_\gamma 915.9 \equiv 100$). Moreover, a spin of $\frac{17}{2}$ would require the 685.9 keV transition to be a stretched quadrupole. However, the A_2/A_0 value listed in Table I for the 685.9 keV transition is not the value of $+0.29$ expected for a stretched quadrupole assignment. Therefore, $J^\pi = 15/2^+$ is probably the correct assignment; the systematics of this level is discussed below. In addition to the main cascade, Fig. 5 also shows for completeness two transitions found previously from a study[5] of the β^+-EC decay of ^{99}Cd. The second excited state is a $J^\pi = 1/2^-$ β-decaying isomer. Two additional states of low spin, not shown in Fig. 5, have also been found.[5]

The assignments for the levels of ^{100}Cd up to $J^\pi = 8^+$ seem straightforward based on the angular distribution results listed in Table II. These data represent the first evidence for the multipolarity of these transitions apart from the lifetime measurement of the 8^+ level by Alber

TABLE II. Transitions in ^{100}Cd. The relative γ-ray intensities are obtained from γ-γ coincidence data and have been corrected for the efficiencies of the germanium detectors. The angular distribution results are obtained from neutron gated spectra and include a small correction for the finite solid angle of the detector.

E_γ (keV)	I_γ	A_2/A_0	A_4/A_0	Assignment
296.27±0.17	92±9	+0.46±0.28	≡0	$8^+ \rightarrow 6^+$
452.56±0.17	36±19	+0.17±0.37	≡0	$6^+ \rightarrow 4^+$
795.02±0.21	≡90±22	+0.52±0.26	≡0	$4^+ \rightarrow 2^+$
1004.03±0.17	104±9 [a,b]	+0.36±0.17 [b]	≡0	$2^+ \rightarrow 0^+$

[a]Value obtained from angular distribution data.
[b]Value may be perturbed by an unresolved transition.

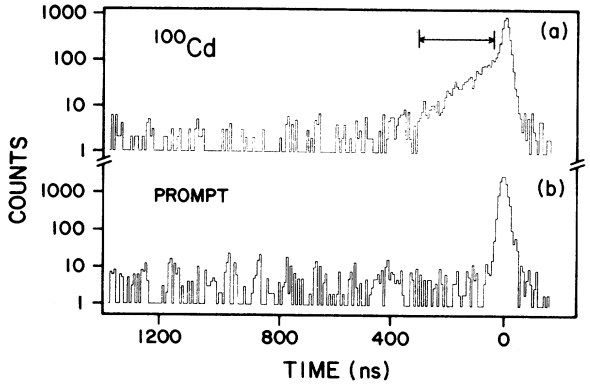

FIG. 7. (a) The summed spectrum of three background-subtracted gates set on transitions assigned to ^{100}Cd, 1004.0, 795.0, and 452.6 keV, obtained from neutron-γ ray coincidence data. The range of data utilized to obtain the half-life of the $J^{\pi}=8^{+}$ level of ^{100}Cd is indicated. (b) Similarly for several prompt transitions of similar energies in other nuclei.

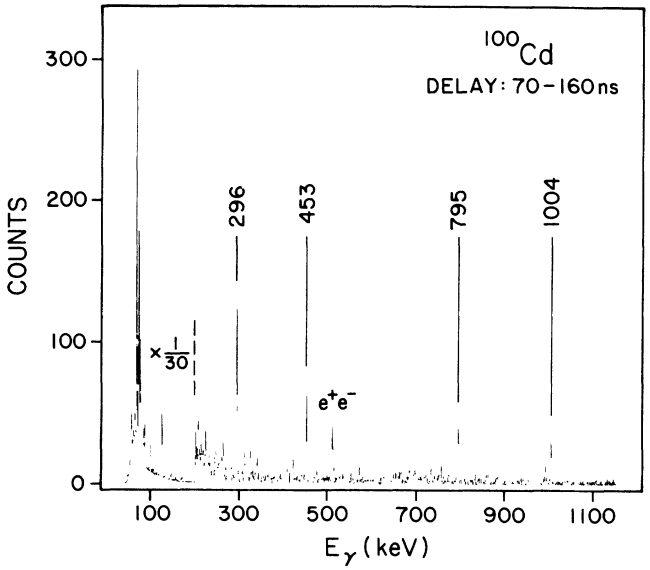

FIG. 8. Delayed γ rays following 167 MeV ^{40}Ca+^{64}Zn. The transitions previously assigned to ^{100}Cd by Alber *et al.* (Ref. 4) are indicated.

et al.[4] which indicated that the 296.3 keV transition is of electric quadrupole multipolarity.

A search for isomeric levels in both ^{99}Ag and ^{100}Cd was made by recording the time delays between neutrons striking any NE213 detector and γ rays striking a germanium detector. The time resolution, with the neutron detectors located 10 cm downstream from the target, was determined to be 20 ns (FWHM). No new isomers with a half-life larger than 5 ns were found in ^{99}Ag, although the sensitivity of the method decreases somewhat for the weaker transitions. The TAC spectra for the 1004.0-, 795.0-, and 452.6-keV transitions in ^{100}Cd were found to be similar and the summed spectrum is shown in Fig. 7(a). The spectrum for the 296.3 keV transition has a slightly different shape, presumably due to electronic triggering effects on this lower energy transition, and was, therefore, omitted from the summed spectrum. Fig. 7(b) shows for comparison the summed response for six prompt transitions in other nuclei. The average half-life obtained from separate fits to the three lowest ^{100}Cd transitions is 73±5 ns. The range of the fit covers 3.7 half-lives as shown in Fig. 7(a). The time calibration was obtained by recording the LINAC beam bursts which occur every 106.4 ns. The half-life is slightly longer than the value of 40^{+20}_{-10} ns found by Alber *et al.*[4] and corresponds to an $E2$ transition strength of 0.121±0.009 W.u. (where W.u. denotes Weisskopf units) as listed in Table III. The four ^{100}Cd transitions are shown in Fig. 8 where only transitions delayed from 70 to 160 ns with respect to a coincident neutron are shown.

IV. DISCUSSION

Since the present study reports the first data for the high-spin states of ^{99}Ag and complements a recent report for ^{100}Cd, one expects future experiments to probe these levels in more detail. In the following discussion of the nuclear structures, therefore, we rely on the systematic behavior found for the lighter isotones. First, the odd-A levels are discussed, followed by those in the even-A nuclei. Finally, several of the more recent structure calculations are mentioned.

A. Odd-A levels

It is worthwhile to compare the present results for ^{99}Ag with what has been found for the isotones ^{95}Tc and ^{97}Rh (Refs. 9 and 2) as shown in Fig. 9. Interestingly, a $J^{\pi}=11/2^{+}$ state in ^{95}Tc has been found at slightly higher excitation energy ($\Delta E=75$ keV) than the yrast $13/2^{+}$ level. These two levels are probably the $J_{\max}$ and $J_{\max}-1$ members of the $\pi g_{9/2}\times 2^{+}$ multiplet for the yrast 2^{+} state in ^{94}Mo. In addition, ^{95}Tc exhibits a closely spaced pair of yrast levels near 1.5 MeV with $J^{\pi}=15/2^{+}$ and $17/2^{+}$ where the $15/2^{+}$ level is slightly higher ($\Delta E=34$ keV) than the $17/2^{+}$ level. These latter two levels are likely the $J_{\max}$ and $J_{\max}-1$ members of $\pi g_{9/2}\times 4^{+}$. Thus, for both multiplets in ^{95}Tc, the $J_{\max}$ member lies below the $J_{\max}-1$ member. This behavior

TABLE III. The empirical $8^{+}\rightarrow 6^{+}$ transition strengths in the $N=52$ isotones. The calculated $E2$ single particle lifetimes are listed in the fifth column for comparison.

Nuclide	E_{γ} (keV)	$t_{1/2}$ (ns)	Branching (%)	$t^{\text{s.p.}}_{1/2}$ (ns)	$B(E2,8^{+}\rightarrow 6^{+})$ W.u.
^{92}Zr	351.3	1.18±0.07	100	4.22	3.58
^{94}Mo	532.4	98±2	76.8	0.512	0.004 00
^{100}Cd	296.3	73±5	100	8.84	0.121

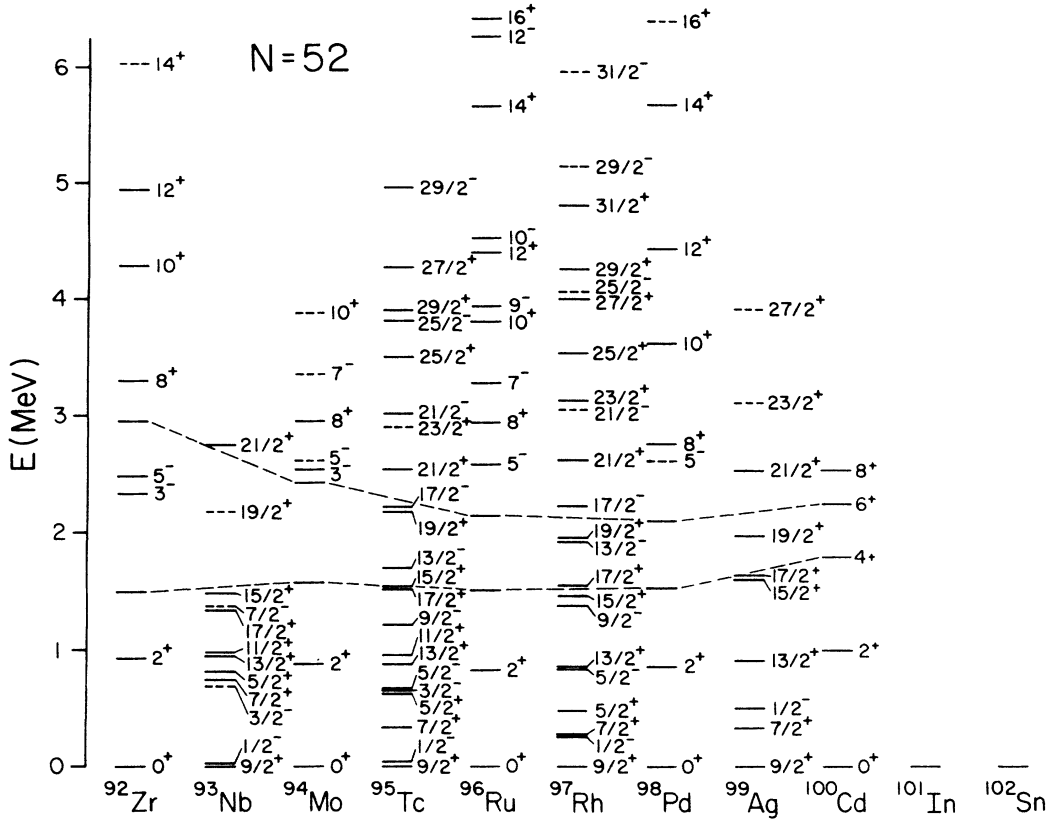

FIG. 9. Yrast states of $N=52$ nuclides ranging from ^{92}Zr to ^{102}Sn. The dashed lines connecting the 4^+ and 6^+ levels are meant to guide the eye, as discussed in the text.

is characteristic of a particle-particle like interaction between the valence proton and neutron configurations. By contrast, the yrast $17/2^+$ state of ^{99}Ag shown in Fig. 9 lies just above ($\Delta E=43$ keV) the $15/2^+$ state, both suggesting a hole-particle interaction between the $\nu=1$ proton configuration and the $\nu=2$ neutron configuration and continuing the behavior found for ^{97}Rh. Since, in the shell model, ^{97}Rh and ^{99}Ag lie above the middle of the $Z=38-50$ shell while ^{95}Tc lies just below, this reversal of the excitation energies of the $15/2^+$ and $17/2^+$ states is not surprising. Unfortunately, the location of the yrast $11/2^+$ level of ^{99}Ag could not be determined from the present data. The location of this level, which is expected to lie slightly below the $13/2^+$ level, would have further documented the interaction. However, in the isotone ^{93}Nb the yrast $13/2^+$ level does lie slightly below ($\Delta E=29$ keV) the $11/2^+$ level as expected for a particle-particle type interaction.

It is seen in Fig. 9 that the excitation energies of the yrast $21/2^+$ levels are similar from ^{93}Nb to ^{99}Ag, suggesting a related structure. The ^{93}Nb level is thought to be $\pi p^2_{1/2}g_{9/2}\nu d_{5/2}g_{7/2}$ relative to an inert ^{88}Sr core. This assignment is based on the result[10] that this level is fed by a moderately fast β decay, with log $ft=5.05\pm0.08$, of a $21/2^+$ level in ^{93}Mo. The parent level is attributed to $\pi p^2_{1/2}g^2_{9/2}(8^+)\nu d_{5/2}$ and the beta transition to $\pi g_{9/2}\rightarrow\nu g_{7/2}$. The empirical value of log ft fits nicely into the range of 4.9 to 5.2 found for this type of transition between odd-A nuclides in this mass region.

The yrast $7/2^+$ levels of ^{99}Ag and ^{95}Tc are found at similar excitation energies. The ^{95}Tc state has been found in (p,n) data but has not been seen in proton stripping reactions, suggesting that it is a three-quasiparticle state. Moreover, the ^{95}Tc level is populated by a moderately fast β decay, with log $ft=5.25$, of the $5/2^+$ ground state of ^{95}Ru. Therefore, the ^{95}Tc level must be primarily $\pi p^2_{1/2}g^3_{9/2}(\nu=1)\nu d_{5/2}g_{7/2}$. This is based on the assumption that the parent ^{95}Ru state is $\pi p^2_{1/2}g^4_{9/2}(0^+)\nu d_{5/2}$ and that the β decay proceeds by $\pi g_{9/2}\rightarrow\nu g_{7/2}$. Therefore, any future collective calculations, such as a particle-vibrator coupling model or an interacting-boson–fermion-approximation model, should not attempt to describe the yrast $7/2^+$ level of ^{95}Tc as a $g_{9/2}$ proton coupled to the 2^+ level of either ^{94}Mo or ^{96}Ru. This conclusion is based on the assumption that both 2^+ states are primarily $\pi p^2_{1/2}g^n_{9/2}(0^+)\nu d^2_{5/2}(2^+)$.

B. Even-A levels

The ^{100}Cd levels with positive parity are in agreement with the systematic behavior of the lighter $N=52$ nuclides as shown in Fig. 9. It can be seen that the excitation energy of the 6^+ level decreases near the middle of the $g_{9/2}$ shell and begins to rise again in ^{100}Cd. This behavior suggests that the 6^+ states of both ^{96}Ru and ^{98}Pd

contain a significant collective component. The energies of the 2^+ and 4^+ levels, however, are more nearly constant across the shell, suggesting a $\pi p^2_{1/2} g^n_{9/2}(0^+) \nu d^2_{5/2}(\nu=2)$ structure relative to an inert ^{88}Sr inert core. One difficulty with this latter interpretation, however, is that the value[11] of -0.03 ± 0.05 found for the g factor of the 2^+ level of ^{92}Zr is smaller in magnitude than the value of -0.37 expected for a $\nu d^2_{5/2}$ structure. This discrepancy might be due to admixtures of $\pi g^2_{9/2}$, $\nu d_{5/2} s_{1/2}$, or $\nu d_{3/2} d_{5/2}$.

The yrast 6^+ levels of ^{94}Mo and ^{100}Cd shown in Fig. 9 are found at similar excitation energies. The ^{94}Mo level is fed by a moderately fast β decay, with log $ft=5.06$, of the 7^+ ground state of ^{94}Tc. The empirical g factor of the ^{94}Tc ground state is consistent with a pure $\pi p^2_{1/2} g^3_{9/2}(\nu=1) \nu d_{5/2}$ structure, although the presence of a modest amount of $\pi p^2_{1/2} g^3_{9/2}(\nu=1) \nu g_{7/2}$ cannot be ruled out. This conclusion is based on the assumption that additivity holds for the separate odd-neutron and odd-proton g factors. Since the β decay must proceed by the $\pi g_{9/2} \rightarrow \nu g_{7/2}$ transition, the ^{94}Mo 6^+ level must be predominantly $\pi p^2_{1/2} g^2_{9/2}(0^+) \nu d_{5/2} g_{7/2}$. Finally, the yrast 8^+ level of ^{100}Cd shown in Fig. 9 is slightly lower lying than the 8^+ level of ^{94}Mo. The g factor of the ^{94}Mo level has been found to be consistent with a $\pi p^2_{1/2} g^2_{9/2}(8^+) \nu d^2_{5/2}(0^+)$ structure. The $8^+ \rightarrow 6^+$ reduced transition strengths in the $N=52$ isotones are summarized in Table III, including the present measurement for ^{100}Cd. The hindered $B(E2)$ value found for ^{94}Mo is seen to be in agreement with the proposal that the 8^+ level is primarily due to proton excitation while the 6^+ level is due to neutron excitation. However, the analogous transition in ^{100}Cd is seen to be 30 times faster than in ^{94}Mo.

We wish to display the yrast 2^+ and 4^+ levels in ^{100}Cd in the framework of the two-parameter VMI equations

$$E_J = \frac{C}{2}(\mathcal{J}-\mathcal{J}_0)^2 + \frac{J(J+1)}{2\mathcal{J}} , \tag{2}$$

and

$$\frac{\delta E_J}{\delta \mathcal{J}} = 0 , \tag{3}$$

where C and $\mathcal{J}_0$, the stiffness and the ground state deformation parameters, can be determined from the quantities E_2 and E_4, the excitation energies of the 2^+ and 4^+ levels. Fig. 10 shows the variation of E_2 and $R_4=E_4/E_2$ with the neutron number for the even-even $_{46}$Pd, $_{48}$Cd, $_{50}$Sn, $_{52}$Te, and $_{54}$Xe nuclides. The three horizontal lines in Fig. 10(b) refer to: the rotational limit at $R_4=3.333$; the line of $\mathcal{J}_0=0$ indicating maximum softness $\sigma=1/(2C\mathcal{J}_0^3)$ at $R_4=2.23$; and the line of $\mathcal{J}_0=-\infty$ at $R_4=1.82$ where nuclei reach maximum hardness when a shell is closed. According to the values for ^{100}Cd, $E_2=1.0040$ MeV and $R_4=1.792$, this nuclide lies near to the line of maximum hardness. The VMI value[12,13] for the energy of the 6^+ level is 2.656 MeV, i.e., 404 keV above the observed value of 2.2516 MeV, and 3.478 MeV for the 8^+ level, i.e., 930 keV above the observed value of 2.5479 MeV. Therefore, the $J^\pi=6^+$ and 8^+ levels of ^{100}Cd lie below the VMI predictions, continuing the trend found previously for 2p-2h nuclei. The VMI (or Mallman) curves are shown, for example, in Fig. 2 of Ref. 3.

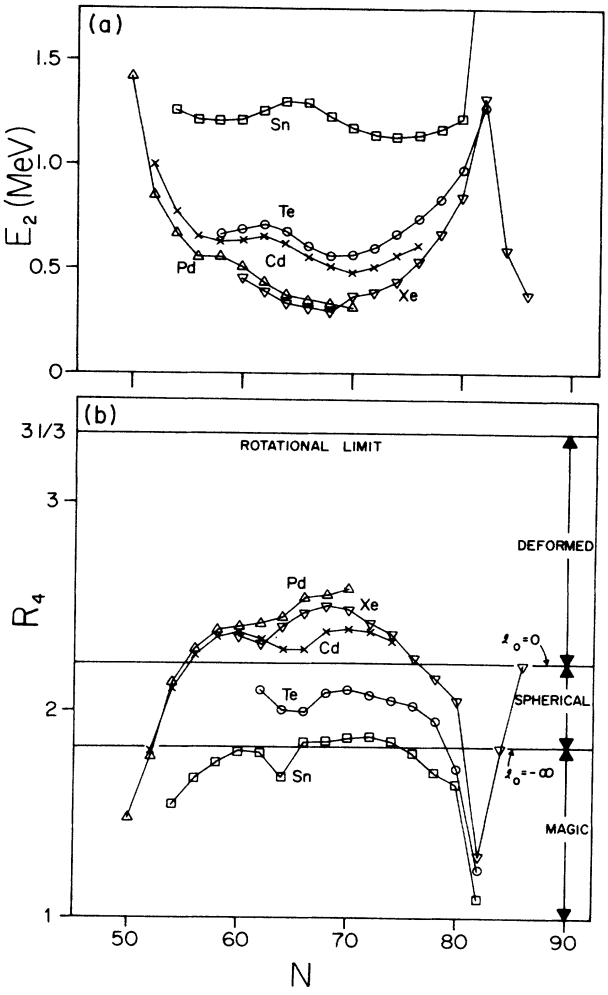

FIG. 10. The empirical E_2 and $R_4=E_4/E_2$ values in the framework of the VMI equations for the even-even nuclides with $Z=46\rightarrow54$ and $N=50\rightarrow82$.

C. Previous calculations

The even-parity states of ^{95}Tc and ^{94}Mo have been calculated by Skouras and Dedes using a shell model[14] with only one free parameter, the effective charge. The valence particles outside of a ^{90}Zr core were: $\pi g_{9/2}$, $\nu d_{5/2}$, $\nu s_{1/2}$, $\nu d_{3/2}$, and $\nu g_{7/2}$. Minehara and Mitarai have calculated the low-lying positive parity levels of ^{95}Tc by using a particle-rotation coupling model.[15] Reinhardt has calculated[16] the energy levels and $B(E2)$ values for the $\pi g_{9/2} \times 2^+$ multiplet in ^{93}Nb.

The yrast 2^+ and 4^+ levels of ^{92}Zr, considered as two-quasineutron states within the framework of a quasiparticle-phonon model, have been calculated by Soloviev *et al.*[17] They find that for the 2^+ level of ^{92}Zr the only significant admixture to $\nu d^2_{5/2}$ is $\nu d_{5/2} s_{1/2}$ where the model space included: $\nu d_{5/2}$, $\nu s_{1/2}$, $\nu d_{3/2}$,

$\nu h_{11/2}$, and $\nu g_{7/2}$. A $\nu d_{5/2}s_{1/2}$ admixture has also been found[18] from an analysis of (d,p) data. The energy levels of ^{92}Zr, ^{94}Mo, and ^{96}Ru have been calculated[19] using the generalized broken-pair approximation. The model space used included the $\pi g_{9/2}$, $\pi p_{1/2}$, $\nu d_{5/2}$, and $\nu s_{1/2}$ orbitals outside of a ^{88}Sr inert core. The levels of ^{98}Pd have been calculated by Sau *et al.*[20] using a shell model of valence particles outside of a ^{100}Sn core. Based on this calculation, it is expected that the yrast 4^+ and 6^+ levels of ^{98}Pd are primarily two-quasineutron excitations while the 8^+ level should be a two-quasiproton state.

Vervier has compared[21] the excitation energies of states with negative parity and spin $J+\frac{1}{2}$ in each of several odd-A nuclides to the energies of states with positive parity and spin J in the corresponding even-even core. This comparison included two pairs of nuclides with $N=52$: ^{94}Mo$-^{95}$Tc and ^{96}Ru$-^{97}$Rh. The relative lowering of the states in the odd-A nuclei was attributed to the existence of a monopole term in the boson-fermion interaction of the interacting boson fermion model.

In summary, new high-spin states of ^{99}Ag have been identified by in-beam γ-ray spectroscopy and the angular distributions and excitation functions of transitions previously assigned to ^{100}Cd have been measured for the first time. Moreover, the half-life of the 8^+ level of ^{100}Cd has been refined and the reduced transition strength shown to be faster than the analogous transition in the isotone ^{94}Mo. A comparison of the yrast positive-parity states of ^{99}Ag with those of the lighter odd-A isotones ^{97}Rh, ^{95}Tc, and ^{93}Nb documents an expected change in the effective interaction of the valence protons with the two valence neutrons above $N=50$. The present study of ^{99}Ag and ^{100}Cd indicates that the availability of new arrays of detectors and the use of new techniques can be expected to facilitate spectroscopic studies in this largely unexplored mass region.

This work was supported in part by the National Science Foundation.

*Permanent address: Institute of Atomic Energy, Beijing, People's Republic of China.

[1]W. F. Piel, Jr. and G. Scharff-Goldhaber, Phys. Rev. C **30**, 902 (1984).
[2]W. F. Piel, Jr., G. Scharff-Goldhaber, C. J. Lister, and B. J. Varley, Phys. Rev. C **33**, 512 (1986).
[3]G. Scharff-Goldhaber, J. Phys. (London) **G5**, L207 (1979); Corrigendum **G6**, 413 (1980).
[4]D. Alber, H. Grawe, H. Haas, B. Spellmeyer, and X. Sun, Z. Phys. **A327**, 127 (1987).
[5]A. W. B. Kalshoven, F. W. N. De Boer, W. H. A. Hesselink, S. Idzenga, J. Ludziejewski, F. Ottenhof, J. J. Van Ruyven, H. Verheul, A. Knipper, G. Marguier, C. Richard-Serre, B. Bergersen, E. Hagebø, and Ø. Scheidemann, Nucl. Phys. **A337**, 120 (1980).
[6]W. Kurcewicz, E. F. Zganjar, R. Kirchner, O. Klepper, E. Roeckl, P. Komninos, E. Nolte, D. Schardt, and P. Tidemand-Petersson, Z. Phys. A **308**, 21 (1982).
[7]F. Puhlhofer, Nucl. Phys. **A280**, 267 (1977).
[8]L. Hildingsson, C. W. Beausang, D. B. Fossan, W. F. Piel, Jr., A. P. Byrne, and G. Dracoulis, Nucl. Instrum. and Methods **A252**, 91 (1986).
[9]K. A. Marshall, J. V. Thompson, W. B. Cook, and M. W. Johns, Can. J. of Phys. **56**, 117 (1978).
[10]R. A. Meyer and R. P. Yaffe, Phys. Rev. C **15**, 390 (1977).
[11]M. Hass, C. Broude, Y. Niv, and A. Zemel, Phys. Rev. C **22**, 1065 (1980).
[12]G. Scharff-Goldhaber, J. Phys. (London) **A7**, L121 (1974).
[13]G. Scharff-Goldhaber, C. Dover, and A. L. Goodman, Ann. Rev. Nucl. Sci. **26**, 239 (1976).
[14]L. D. Skouras and C. Dedes, Phys. Rev. C **15**, 1873 (1977); Phys. Lett. **66B**, 417 (1977).
[15]E. Minehara and S. Mitarai, J. Phys. Soc. Japan **48**, 4 (1980).
[16]H. Reinhardt, Nucl. Phys. **A337**, 176 (1980).
[17]V. G. Soloviev, O. Stoyanova, and V. V. Voronov, Nucl. Phys. **A370**, 13 (1981).
[18]T. Borello-Lewin, H. M. A. Castro, L. B. Horodynski-Matsushigue, and O. Dietzsch, Phys. Rev. C **20**, 2101 (1979).
[19]Y. K. Gambhir, S. Haq, and J. K. Suri, Ann. Phys. (N.Y.) **133**, 154 (1981).
[20]J. Sau, K. Heyde, and J. Van Maldeghem, Nucl. Phys. **A410**, 14 (1983).
[21]J. Vervier, Phys. Lett. **149B**, 267 (1984).